



Performance analysis a of solar driven organic Rankine cycle using multi-component working fluids

Baldasso, E.; Andreasen, J. G.; Modi, A.; Haglind, F.; Stoppato, A.

Published in:
Proceedings of ECOS 2015

Publication date:
2015

Document Version
Publisher's PDF, also known as Version of record

[Link back to DTU Orbit](#)

Citation (APA):

Baldasso, E., Andreasen, J. G., Modi, A., Haglind, F., & Stoppato, A. (2015). Performance analysis a of solar driven organic Rankine cycle using multi-component working fluids. In Proceedings of ECOS 2015: 28th International Conference on Efficiency, Cost, Optimization, Simulation and Environmental Impact of Energy Systems

General rights

Copyright and moral rights for the publications made accessible in the public portal are retained by the authors and/or other copyright owners and it is a condition of accessing publications that users recognise and abide by the legal requirements associated with these rights.

- Users may download and print one copy of any publication from the public portal for the purpose of private study or research.
- You may not further distribute the material or use it for any profit-making activity or commercial gain
- You may freely distribute the URL identifying the publication in the public portal

If you believe that this document breaches copyright please contact us providing details, and we will remove access to the work immediately and investigate your claim.

Performance analysis a of solar driven organic Rankine cycle using multi-component working fluids

E. Baldasso^a, J. G. Andreasen^b, A. Modi^c, F. Haglind^d and A. Stoppato^e

^aUniversity of Padova, Padova, Italy, baldassoenrico@gmail.com(CA)

^bTechnical University of Denmark, Kgs. Lyngby, Denmark, jgan@mek.dtu.dk

^cTechnical University of Denmark, Kgs. Lyngby, Denmark, anmod@mek.dtu.dk

^dTechnical University of Denmark, Kgs. Lyngby, Denmark, frh@mek.dtu.dk

^eUniversity of Padova, Padova, Italy, anna.stoppato@unipd.it

Abstract:

Among the different renewable sources of energy, solar power could play a primary role in the development of a more sustainable electricity generation system. While large scale concentrated solar power plants based on the steam Rankine cycle have already been proved to be cost effective, research is still under progress for small scale low temperature solar-driven power plants. The steam Rankine cycle is suitable for high temperature applications, but its efficiency drastically decreases as the heat source temperature drops. In these cases a much more promising configuration is the organic Rankine cycle. The purpose of this paper is to optimize a low temperature organic Rankine cycle tailored for solar applications. The objective of the optimization is the maximization of the solar to electrical efficiency and the optimization parameters are the working fluid and the turbine inlet temperature and pressure. Both pure fluids and binary mixtures are considered as possible working fluids and thus one of the primary aims of the study is to evaluate whether the use of multi-component working fluids might lead to increased solar to electrical efficiencies. The considered configuration includes a solar field made of parabolic trough collectors and a recuperative organic Rankine cycle. Pressurized water is selected as heat transfer fluid and its maximum temperature is fixed to 150°C. The target power output for the plant is 100 kW_{el}. A part load analysis is carried out in order to define the most suitable control strategy and both the overall annual production and the average solar to electrical efficiency are estimated with an annual simulation. The results suggest that the introduction of binary working fluids enables to increase the solar system performance both in design and part-load operation.

Keywords:

Organic Rankine cycles, Zeotropic mixtures, Solar power plants, Part-load.

1. Introduction

Solar based power plants are promising in those locations characterised by high values of the direct normal irradiation (DNI) and thus much research has been carried out in this field [1,2]. Different solar field and power cycle technologies have been investigated. The biggest parabolic trough application is the Solar Electric Generation System (SEGS) located in southern California and has an overall capacity of 354 MW_{el} [3]. The SEGS power plants are connected to steam Rankine cycles and have proved the cost-effectiveness of this solution for large scale, high temperature applications. Conversely, the profitability of small scale, low temperature concentrated solar power (CSP) plants is still under investigation. When the heat source temperature decreases the efficiency of the steam power plant decreases and a much more promising configuration is the organic Rankine cycle (ORC) [4]. As reported by Quoilin et al. [5] few solar systems operate with an ORC: a 1 MW_{el} power plant using n-pentane is located in Arizona, a 100 kW_{el} system was commissioned

in Hawaii and some kW-size prototypes are under study for remote off-grid applications. The choice of a proper working fluid plays an essential role in the development of an efficient and cost-effective ORC. The selected organic compound has a huge impact on some of the most important characteristics of the power plant: performance and cost of cycle components, system stability, safety and environmental impact [6]. The choice of a proper working fluid is affected by many factors: the characteristics of the available heat source, the size of the plant and the current legislation, and therefore every new power plant has to be analysed on its own.

The use of ORCs for the exploitation of low temperature heat sources leads to efficiency improvements compared to steam Rankine cycles, but still there are some limitations related to the fact that the isothermal boiling process creates a non-optimal thermal match between the heat source fluid and the working fluid which results in large irreversibilities [7]. A possible solution for reducing the irreversibilities in the evaporation process is the introduction of a supercritical cycle, which is characterised by a non-isothermal phase shift. On the other hand, as reported by Chen et al. [8], supercritical cycles usually require higher working pressures and therefore difficulties in the plant operation and safety concerns might appear. Another possibility is the introduction of binary zeotropic working fluids. This concept enables both to take advantage of the non-isothermal phase change process and to avoid the problems related to the high operating pressures. In this case the non-isothermal phase shift is related to the unequal concentration of the liquid and vapour phase during the phase change process, taking place both in the evaporator and in the condenser. Moreover, Chen et al. [7] showed that mixtures can be effectively used even in supercritical configurations, leading to lower exergy destruction both in the condenser and in the boiler. According to their study, when the heat source temperature is 410 K, a supercritical cycle using a R134a/R32 (0.7/0.3) zeotropic mixture improves the exergy efficiency of the condensation process and of the heating process by 22.67 % and 7.30 %, respectively, compared to an ORC using pure R134. Moreover, the authors recommend that a zeotropic mixture to be used in supercritical configurations should have a thermal glide during the condensation process in order to take advantage of the non iso-thermal condensation.

The majority of the ORC studies on mixtures consider a geothermal heat source and aim at the maximization of the cycle net power output. Heberle et al. [9] showed that the second law efficiency of the best mixture of isobutane and isopentane is 8 % higher than the one for pure isobutane. Andreasen et al. [10] proposed a generic methodology for ORC optimization. The result indicated that the introduction of binary working fluids can lead to higher power productions and to lower pressure levels. When the hot fluid inlet temperature is 120 °C, a mixture of ethane and propane enables to reach a net power output 12.9 % higher than pure ethane. Braimakis et al. [11] analysed the use of refrigerant mixtures for low temperature waste heat recovery systems. Their study indicated that both pure propane and a mixture of propane/butane exhibit better thermodynamic performance and favourable size parameter, volume flow ratio and turbine volume flow rate compared to pure R245fa. Zhao and Bao [12] investigated the effect of composition shift in organic Rankine cycles using zeotropic mixtures. The study showed that composition shift significantly influences the performance of organic Rankine cycles leading to a lower net power output and thermal efficiency. Wang et al. [13] conducted an experimental study of a low-temperature solar Rankine cycle system and showed that zeotropic mixtures have the potential to increase the overall system efficiency. According to their study, the use of a mixture of R245fa/R152a (0.7/0.3) enables to reach an average overall efficiency of 1.28 %, while the efficiency is 0.88 % when using pure R152a. Mavrou et al. [14] investigated the annual performance of a low temperature ORC system using flat plate collectors and thermal storage. The highest power output and thermal efficiency in their analysis were obtained with a mixture of neopentane/2-fluoromethoxy-2-methylpropane (0.7/0.3)

Table 1. List of considered working fluids

Fluid	Category	$T_c(^{\circ}\text{C})$	$p_c(\text{bar})$	ODP	GWP
n-butane	Natural ref.	151.98	37.96	0	4
cyclohexane	Cyclo alkanes	280	40.7	n.a.	n.a.
cyclopentane	Cyclo alkanes	238.55	45.1	0	<25
n-hexane	Alkanes	236	30.6	0	0
iso-hexane	Cyclo alkanes	225	30.4	n.a.	n.a.
Iso-pentane	Alkanes	187	33.7	0	0
Iso-butane	Hydrocarbons	135	36.4	0	20
n-pentane	Alkanes	196.5	33.6	0	20
R1234yf	HFO	94.7	33.82	0	4
R1234ze	HFO	109.4	36.36	0	6

A model of the solar field is derived using Engineering Equation Solver (EES) [22], following the method suggested by Forristal [23]. In the present study the heat losses through the support brackets ($\dot{q}'_{cond,bracket}$) are neglected since they are low compared with the other heat fluxes, especially at low temperatures. Moreover, two additional heat fluxes ($\dot{q}'_{4,SolAbs}$ and $\dot{q}'_{Sol,Refl}$) are introduced. The former considers the solar energy that is transmitted through the protective glass, reflected back from the absorber element and absorbed into the inner surface of the glass; the latter takes into account the solar energy that is reflected back into the environment and thus does not participate to the overall energy balance. The various heat fluxes are depicted in Fig. 2. The energy balances considered in the current model are:

$$\dot{q}'_{12,conv} = \dot{q}'_{23,cond} , \quad (2)$$

$$\dot{q}'_{3,SolAbs} = \dot{q}'_{34,conv} + \dot{q}'_{34,rad} + \dot{q}'_{23,cond} , \quad (3)$$

$$\dot{q}'_{34,conv} + \dot{q}'_{34,rad} + \dot{q}'_{4,SolAbs} = \dot{q}'_{45,cond} , \quad (4)$$

$$\dot{q}'_{45,cond} + \dot{q}'_{5,SolAbs} = \dot{q}'_{56,conv} + \dot{q}'_{57,rad} , \quad (5)$$

$$\dot{q}'_{heat,Loss} = \dot{q}'_{56,conv} + \dot{q}'_{57,rad} + \dot{q}'_{Sol,Refl} , \quad (6)$$

where $\dot{q}'_{12,conv}$ is the convective heat flux between the heat transfer fluid and the inner surface of the absorber, $\dot{q}'_{23,cond}$ is the conductive heat flux between the inner and the outer surface of the absorber, $\dot{q}'_{34,conv}$ is the convective heat flux between the outer surface of the absorber and inner surface of the protective glass, $\dot{q}'_{34,rad}$ is the radiative heat flux between the outer surface of the absorber and inner surface of the protective glass, $\dot{q}'_{cond,bracket}$ is the conductive loss through the support brackets, $\dot{q}'_{45,cond}$ is the conductive heat flux between the inner and the outer surface of the protective glass, $\dot{q}'_{56,conv}$ is the convective heat flux between the outer surface of the protective glass and the environment, $\dot{q}'_{57,rad}$ is the radiative heat flux between the outer surface of the protective glass and the environment, $\dot{q}'_{3,SolAbs}$ is the solar irradiation absorbed by the outer surface of the absorber and $\dot{q}'_{5,SolAbs}$ is the solar irradiation absorbed by the outer surface of the protective glass. The various heat fluxes are estimated using the same heat transfer correlations proposed by Forristal [23]. The heat fluxes related to the solar radiation are calculated as follows:

$$\dot{q}'_{SolAbs} = DNI \cdot \cos(\theta) \cdot IAM \cdot A_p \cdot \eta_{opt} , \quad (7)$$

$$\dot{q}'_{5,SolAbs} = \dot{q}'_{SolAbs} \alpha_{gl} , \quad (8)$$

$$\dot{q}'_{4,SolAbs} = \dot{q}'_{SolAbs} \frac{\tau_{gl} \alpha_{gl} (1 - \alpha_{abs})}{1 - \rho_{gl} (1 - \alpha_{abs})}, \quad (9)$$

$$\dot{q}'_{3,SolAbs} = \dot{q}'_{SolAbs} \frac{\tau_{gl} \alpha_{abs}}{1 - \rho_{gl} (1 - \alpha_{abs})}, \quad (10)$$

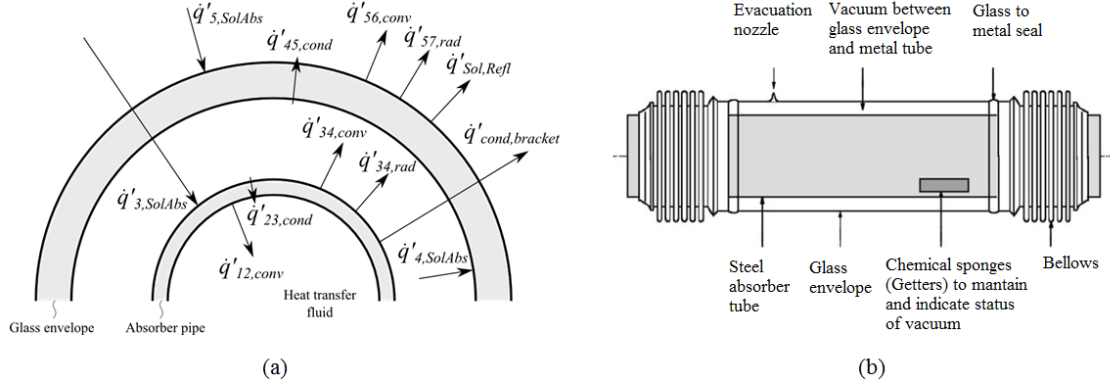


Fig.2. Solar field: (a) considered heat fluxes (b) a shortened view of the receiver [15]

The incidence angle modifier (IAM) is calculated as proposed by Dudley et al. [24], while the incidence angle is estimated considering a north south orientation of the parabolic trough system [25]. The incidence angle is calculated as:

$$\cos(\theta) = \sqrt{\cos^2(\theta_z) - \cos^2(\delta) \sin^2(\omega)}, \quad (11)$$

The validation of the current model was performed by changing the heat transfer correlations and the heat transfer fluid in order to compare the results with the model of Burkholder et al. [15]. The obtained results showed a maximum difference of 1.3 %. The solar field model is fitted with a regression curve obtained with DataFit 9.0 ($R^2 = 99.99\%$) [26] and subsequently included in the ORC model. The pressure losses along the solar field pipelines are estimated following the procedure used by Quoilin et al. [27]. The power system is optimized in design conditions in order to maximize the overall solar to electrical efficiency, which is defined as:

$$\eta_{overall} = \frac{\dot{W}_{plant}}{DNI \cdot S_{tot}} = \frac{\dot{W}_{cycle} - \dot{W}_{sf,pump}}{DNI \cdot S_{tot}}, \quad (12)$$

where $\dot{W}_{sf,pump}$ is the electrical power absorbed by the solar field pump, DNI is the direct normal irradiation and S_{tot} is the solar field surface area. The cycle efficiency is calculated as follows:

$$\eta_{cycle} = \frac{\dot{W}_{cycle}}{\dot{m}_w (h_{hf,in} - h_{hf,out})}, \quad (13)$$

The optimization process is carried out with the genetic algorithm available in the Matlab optimization toolbox. For every couple of working fluids the mixture composition, the cycle maximum pressure and turbine inlet temperature (TIT) are optimized. The cycle maximum pressure is left free to vary between 1 and 40 bar, while the considered range for the TIT is 60-140 °C. The mixture composition is described by means of the mass fraction of the first component. The optimization is run with a population size of 200 individuals for 200 generations. The parameters

that are fixed are listed in Table 2. The design values for the DNI and the generator efficiency are selected referring to similar studies available in literature [17,27].

A part-load model was also developed. The purpose of the part-load model is to investigate the behaviour of the solar system as the available solar energy decreases. The input parameters for the part-load model are the available DNI, the zenith angle, the hour angle and the declination angle, which vary with the time of the year. The variation of the power output due to the ambient temperature and the wind speed is neglected. In the study, the plant is operated until the decrement of the available DNI results in the violation of the pinch point temperatures or in a negative net power output from the overall system. Recuperator, pre-heater, evaporator (discretized into 3 steps) and super-heater are modelled by means of UA values with the relationships used by Patnode [28], while the turbine is modelled using the Stodola equation [29]. The condensing pressure is maintained at the design value when the system operates in part-load conditions. The part-load performances of the electric generator and turbine are estimated using the relationships presented by Haglind and Elmegaard [30] and Schobeiri [31], respectively. The pump part-load efficiency is obtained from [32]. The input of the part-load model is the solar collected energy per unit of solar field surface area:

$$E_{col} = DNI \cdot IAM \cdot \cos(\theta), \quad (14)$$

The solar field pump is operated so that to keep a constant value for the solar field outlet temperature, while three possible control strategies have been investigated for the ORC:

1. Constant turbine inlet temperature
2. Constant super-heating temperature (difference between T_5 and T_{sv})
3. Constant hot fluid outlet temperature

Table 2. Fixed parameters in the optimization process

Heat transfer fluid	Pressurized water at 8 bar
Absorber type	2008 PTR70
Solar collector	LS-3
IAM	1
Incident angle	0°
Optical efficiency	0.8448
Design DNI	800 W/m ²
Design ambient temperature	25 °C
Design wind speed	2 m/s
Cooling water temperature increase	5 °C
Boiler pinch point temperature, ΔT_{pp}	8 °C
Turbine isentropic efficiency, $\eta_{is,t}$	0.70
Pump isentropic efficiency, $\eta_{is,p}$	0.70
Solar field pump efficiency, $\eta_{SolarField,pump}$	1
Electric generator efficiency, η_{gen}	0.98

Based on the part-load model and the irradiation data for Sevilla (Spain) an annual simulation is carried out in order to analyze the behaviour of the different power plants during a full year of operation. In order to decrease the computational time required for this evaluation the part-load model has been fitted with a regression curve obtained with DataFit 9.0 ($R^2=99.9\%$) and the maximum power output has been set to the design value. The annual analysis is performed only for the best performing pure fluid and mixture and the selected control strategy is the one that enables to have the widest range of operation of the plants. It is however possible that a sub-optimal solution at steady state could result in a better overall annual performance after considering part-load operation.

3. Results

The results of the design case optimizations are depicted in Tables 3 (pure fluids) and 4 (mixtures). The performance increment of the various mixtures is calculated with respect to the best pure fluid among the two fluids in the mixture. The results suggest that the hydrofluoroolefins (R1234ze and R1234yf) are less performing than the other candidates. The hot source outlet temperature is a free parameter in the optimization process and as a consequence the best performing configurations are those where the heat is absorbed at the highest possible temperature level. In this context supercritical configurations are penalised by higher temperature drops which lead to lower cycle efficiencies. On the other hand subcritical configurations, where most of the heat is absorbed during the evaporation process, enable to reach higher values for the overall efficiency. For the hydrocarbons the optimization process results in a temperature drop of the heat source that ranges between 14 and 17°C. In a similar study by Quoilinet al. [27] an optimum value of 15°C has been found for this parameter. When the temperature drop is lower than this value, the power absorbed by the solar field circulating pump increases resulting in a decrement of the overall efficiency. Conversely, higher values for the pressurized water temperature drop are related to less performing power cycles (the heat absorption for the ORC takes place at a lower temperature level). It also appears that the best performing solutions are characterised by higher values of the turbine size parameter (SP) and volume flow ratio (VFR) and thus require more expensive turbines. According to the guidelines provided by Astolfi et al. [33] three stages are required for $VFR > 16$, while two stages are required when $4 < VFR < 16$.

The best configuration that uses a binary working fluid is given by a mixture of cyclohexane and cyclopentane (0.84/0.16); see Table 5. In this case the overall efficiency is 2.27 % higher than the optimized configuration using pure cyclohexane. The efficiency increase results in a reduction of the heat input to the cycle and a decrease in the pressurized water mass flow rate (-4.81 %). This enables a 15 % reduction in the power consumption of the solar field pump.

Table 3. Pure fluids result for the overall system optimization

Fluid	p_5 (bar)	TIT (°C)	$T_{hf,out}$ (°C)	SP (m)	VFR (-)	η_{cycle} (-)	$\eta_{overall}$ (-)
cyclohexane	3.80	140.00	135.94	0.089	19.80	0.1562	0.1193
hexane	5.25	140.00	135.46	0.075	19.27	0.1544	0.1187
iso-hexane	6.38	140.00	135.22	0.067	17.44	0.1546	0.1182
cyclopentane	8.26	140.00	134.70	0.054	14.20	0.1515	0.1159
pentane	11.43	140.00	133.55	0.046	13.93	0.1483	0.1149
iso-pentane	13.53	140.00	132.81	0.042	12.82	0.1483	0.1140
butane	24.85	140.00	122.00	0.029	9.68	0.1360	0.1053
iso-butane	29.07	140.00	111.73	0.027	8.13	0.1297	0.1007
R1234ze	36.99	140.00	89.20	0.029	6.94	0.1178	0.0917
R1234yf	40.00	140.00	83.63	0.028	5.54	0.1133	0.0882

On the other hand the configuration using a mixture is characterised by higher UA values for the heat exchangers, especially for the evaporator (11 %) and for the condenser (47 %) which suggest higher investment costs for the heat exchangers. Furthermore, as shown by Radermacher and Hwang [34] the mixtures are characterised by lower values for the heat transfer coefficients compared to pure fluids thus adding to the heat transfer area requirement of the heat exchangers when using mixtures.

Table 4. Mixtures result for the overall system optimization

Fluid 1	Fluid 2	p_5 (bar)	TIT (°C)	x_I (-)	$T_{hf,out}$ (°C)	SP (m)	VFR (-)	$\eta_{overall}$ (-)	increase (%)
butane	iso-pentane	16.24	140	0.20	130.85	0.039	13.42	0.1148	0.69
cyclohexane	cyclopentane	4.61	140	0.84	135.52	0.082	20.97	0.1220	2.27
cyclohexane	hexane	4.39	140	0.59	135.88	0.081	22.37	0.1203	0.81
cyclohexane	iso-hexane	5.01	140	0.55	135.69	0.078	20.44	0.1217	2.03
cyclohexane	iso-pentane	4.19	140	0.97	135.69	0.086	21.20	0.1212	1.55
cyclohexane	pentane	4.30	140	0.95	135.78	0.085	21.35	0.1216	1.89
cyclopentane	hexane	6.42	140	0.31	135.14	0.067	18.64	0.1201	1.22
cyclopentane	iso-pentane	10.56	140	0.58	134.08	0.049	14.75	0.1181	1.92
cyclopentane	pentane	9.53	140	0.65	134.37	0.051	14.55	0.1169	0.86
hexane	iso-hexane	5.71	140	0.76	135.35	0.072	19.02	0.1191	0.34
hexane	iso-pentane	5.92	140	0.93	135.18	0.072	20.43	0.1206	1.64
hexane	pentane	6.18	140	0.86	135.00	0.070	20.15	0.1209	1.89
iso-hexane	pentane	8.04	140	0.76	134.59	0.060	18.30	0.1205	1.90
iso-hexane	iso-pentane	7.35	140	0.90	134.88	0.063	18.52	0.1203	1.77

Table 5. Parameter comparison between the pure fluid and mixture configurations

Parameter	Unit	cyclohexane	cyclopentane/cylohexane	Δ %
\dot{m}_{wf}	[kg/s]	1.35	1.30	-3.45
\dot{m}_w	[kg/s]	10.61	10.10	-4.81
$\dot{W}_{sf,pump}$	[kW]	1.85	1.58	-14.75
P_{cond}	[bar]	0.18	0.21	+15.41
S_{tot}	[m ²]	1028.71	1008.68	-1.95
\dot{W}_{plant}	[kW]	98.15	98.42	+0.28
η_{cycle}	[-]	0.1562	0.1593	+1.98
$\eta_{overall}$	[-]	0.1193	0.1220	+2.27
$UA_{evaporator}$	[W/K]	35483	39629	+11.68
$UA_{condenser}$	[W/K]	37334	55133	+47.66

Figure 3 shows the results of the part-load analysis carried out for cyclohexane and cyclopentane/cyclohexane. In both cases the relative net power output (defined as the fraction of the design power output) is computed as a function of the collected solar energy for the three control strategies. The plots indicate that the widest operating range is achieved with the constant turbine inlet temperature control strategy. When the super-heating temperature is kept fixed during part-load, the plants can also operate in a wide range of collected solar energy, but the corresponding power production is lower compared to the previous strategy. Lastly the power plants are less flexible when the solar field inlet temperature is kept constant: for this control strategy the minimum required solar collected energy are respectively 640 W/m² and 660 W/m², respectively.

For the constant TIT control strategy, the mixture configuration is able to operate at lower loads: the minimum required collected energy is 140 W/m² (relative power = 8%) while this value increases to 220 W/m² (relative power = 17%) for pure cyclohexane. Nevertheless the minimum load of a power plant is usually related to the minimum acceptable load of the turbine. In the following two analyses the relative power output is constrained to 10 and 15 % in order to investigate the influence of such a minimum limit for the turbine load.

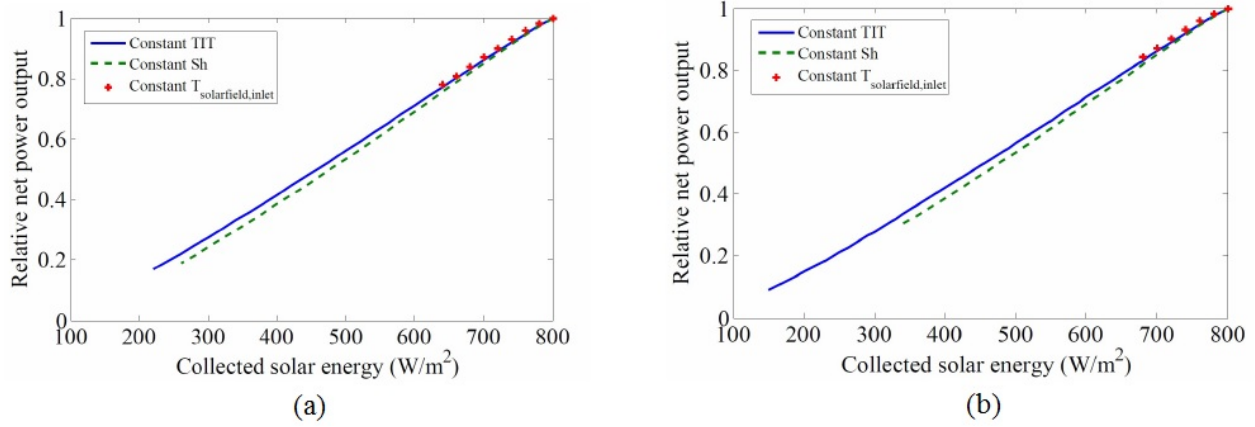


Fig.3. Part load model results: (a) cyclohexane (b) cyclohexane/cyclopentane

The results of the annual simulations, listed in Table 6, suggest an overall annual production of 221.37 MWh for the pure fluid configuration and of 223.44 MWh for the mixture (when the minimum turbine load is set to 15 %). This result amplifies the differences obtained in the design case: the mixture configuration is able to produce more power and is characterised by a higher value for the annual efficiency. The relative increments for these two parameters are respectively 0.95 % and 3 %. The mixture configuration performance further increases when the minimum turbine load is set to 10 %. In this case the annual production reaches 224.83 MWh (1.56 % more than for pure cyclohexane) and the annual efficiency increases by 3.56 % compared to the pure fluid system.

Table 6. Annual simulation results

Configuration	Annual production (MWh)	Annual efficiency	Annual specific production (kWh/m ² year)
Pure fluid	221.31	8.95	215.19
Mixture (min load = 15%)	223.46	9.22	224.54
Mixture (min load = 10%)	224.83	9.27	222.89

Figure 4 shows the variation of the heat exchanger UA values and the turbine efficiency during part-load operation for the first control strategy (constant TIT). The UA value of the pre-heater, evaporator and the super-heater have the same part load variation, thus only the pre-heater is shown in the figures. The variation of the UA value of the recuperator is only related to the decreasing value of the working fluid mass flow rate, while for the pre-heater, evaporator and super-heater the variation is also dependent on the decrease of the pressurized water mass flow rate. The relative decrease in the UA value for the recuperator is therefore less than for the remaining heat exchangers. The part-load performance of the turbine is high in the entire operating range. This is because the part-load efficiency of the turbine is a function of the isentropic enthalpy difference

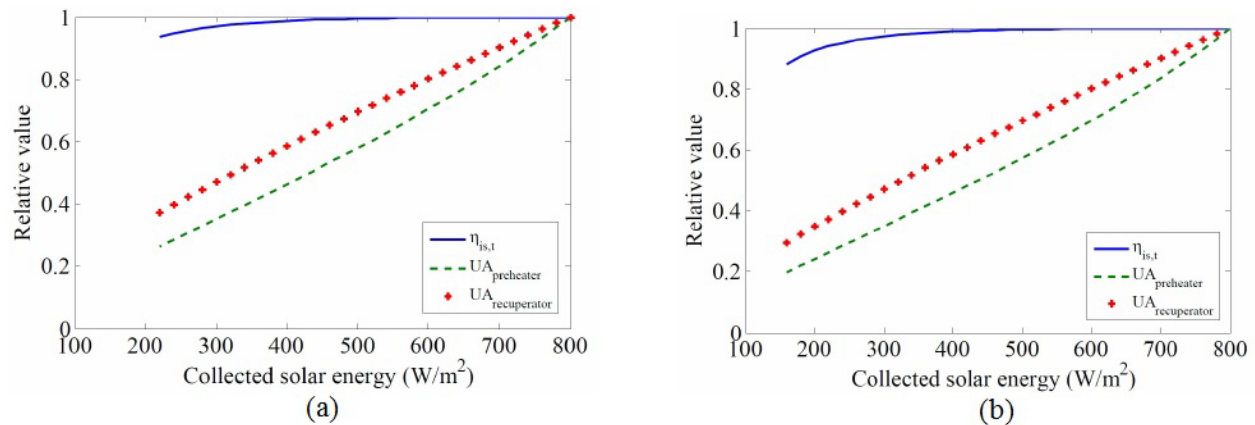


Fig. 4. Variation of $\eta_{is,t}$ and UA during part-load: (a) cyclohexane (b) cyclohexane/cyclopentane

across the turbine, which does not change much during part-load.

4. Conclusions

In this study an overall CSP power plant has been modelled and optimized. The results suggest that a primary factor in the definition of system performance is the temperature decrease of the transfer fluid in the boiler and that its optimum value ranges between 14 and 17 °C. The configurations characterised by lower values of this parameter are penalised by high power absorption for the solar field circulating pump, while the power cycle efficiency decreases when the temperature drop increases (the temperature level at which the heat is absorbed in the cycle decreases and this leads to lower efficiencies). The use of mixtures leads to reduced irreversibility both in the boiler and in the condenser, but is penalised by the lower temperature drop of the heat source. The best performance is reached with a mixture of cyclohexane and cyclopentane (0.84/0.16) which enables to increase the overall system efficiency by 2.27 % compared to the pure cyclohexane configuration. A comparison of these the two fluids suggests that the use of mixtures leads to an increased cycle thermal efficiency which results in a lower circulating mass flow rate in the solar field. This enables to reduce the power absorbed by the solar field circulating pump and thus to reach higher values for the overall efficiency. From an economical point of view the main difference between the two configurations lies in the surface area required for the heat exchangers: the current study suggests that the UA values are higher for the mixture, especially for the condenser (+47 %) and for the boiler (+11 %). Results from an annual simulation indicate that the mixture produces slightly more power than the pure fluid. When the minimum acceptable load is fixed to 15 %, the use of cyclopentane/cyclohexane results in an increment of the annual electricity production by 0.95 % and of the annual efficiency by 3 % compared to pure cyclohexane. Greater performance increments are possible with lower values for the turbine minimum load.

In conclusion, this study suggests that the introduction of binary working fluids in an ORC tailored for solar applications enables to increase the solar system performance both in design and part-load operation. It also appears that the UA values for the heat exchangers are higher for the mixtures, leading to more expensive heat exchangers. Further studies need to be carried out in order to evaluate the use of mixtures from an economic perspective, considering both initial costs and the performance of the CSP plant.

Nomenclature

A_p	collector aperture, m
h	specific enthalpy, kJ/kg
HFC	hydrofluorocarbon
HFO	hydrofluoroolefin
\dot{m}	mass flow rate, kg/s
p	pressure, bar
\dot{q}'	specific heat flux, kW/m
S	surface, m ²
SP	turbine size parameter, m
T	temperature, °C
VFR	turbine volume flow ratio
x	mass fraction
\dot{W}	power, kW

Greek symbols

α	absorptance
δ	declination angle
η	efficiency
θ	incidence angle
θ_z	zenith angle
ρ	reflectance
τ	transmittance
ω	hour angle

Subscripts

abs	absorber
el	electrical
c	critical
coll	collected
gen	generator
gl	glazing
hf	hot fluid
in	inlet
is	isentropic
out	outlet
p	pump
sv	saturated vapour
sf	solar field
t	turbine
w	water
wf	working fluid

References

- [1] Siva Reddy V., Kaushik S.C., Ranjan K.R., Tyagi S.K., State-of-Art of solar thermal power plants - A review. *Renewable and Sustainable Energy Reviews* 2013;27:258-273.
- [2] Kolios A.J., Paganini S., Proja S., Development of thermodynamic cycles for concentrated solar power plants. *International Journal of Sustainable Energy* 2003;32(5):296-314.
- [3] Kearney D.W., Price H.W., Solar thermal plants - Luz concept (current status of the SEGS plants). *Proceedings of the second Renewable Energy Congress; 1992; UK; vol 2:582-588.*
- [4] Saadatfar B., Fakhrai R., Fransson T., Waste heat recovery Organic Rankine cycles in sustainable energy conversion: A state-of-the-art review. *The Journal of Macro Trends in Energy and Sustainability* 2013;1(1):161-188.
- [5] Quoilin S., van der Broek M., Declaye S., D'Elia P., Techno-economic survey of organic Rankine cycle (ORC) systems. *Renewable and Sustainable Energy reviews* 2013;22:166-186.
- [6] Bao J., Zhao L., A review of working fluids and expander selection for organic Rankine cycle. *Renewable and Sustainable Energy reviews* 2013;24:325-342.
- [7] Chen H., Goswami D.Y., Rahman M.M., Stefanos E.K., A supercritical Rankine cycle using zeotropic mixtures working fluids for the conversion of low heat into power. *Energy* 2011;36:549-555.

- [8] Chen H., Goswami D.Y., Stefanos E.K. A review of thermodynamic cycle and working fluids for the conversion of low-grade heat into power. *Renewable and Sustainable Energy Reviews* 2010;14(9):3059-3067.
- [9] Heberle F., Preißinger P., Brüggemann D., Zeotropic mixtures as working fluids in organic Rankine cycles for low-enthalpy geothermal resources. *Energy* 2012;37(1):364-370.
- [10] Andreasen J.G., Larsen U., Knudsen T., Pierobon L., Haglind F., Selection and optimization of pure and mixed working fluids for low grade heat utilization using organic Rankine cycles. *Energy* 2014;73(2014):204-213.
- [11] Bramakis K., Leontaritis A.D., Preißinger M., Karellas S., Brüggerman D. and Panopoulos K., Thermodynamic investigation of waste heat recovery with subcritical and supercritical low-temperature Organic Rankine Cycle based on natural refrigerants and their binary mixtures. ECOS 2014: Proceedings of the 27th ECOS; 2014 Jun 15-19; Turku, Finland.
- [12] Zhao L., Bao J., The influence of composition shift on organic Rankine cycle (ORC) with zeotropic mixtures. *Energy Conversion and Management* 2014;83:203-211.
- [13] Wang J.L., Zhao L., Wang X.D., A comparative study of pure and zeotropic mixtures in low-temperature solar Rankine cycle. *Applied Energy* 2010;87(11):3366-3373.
- [14] Mavrou P., Papadopoulos A.I., Stijepovic M.Z., Steverlis P., Linke P., Voutetakis S., Novel and conventional working fluid mixtures for solar Rankine cycles: Performance assessment and multi-criteria selection. *Applied Thermal Engineering* 2015;75:384-396.
- [15] Burkholder F., Kutscher C., Heat loss testing of Scott's PTR70 parabolic trough receiver. National Renewable Energy Laboratory, Technical report NREL/TP-550-45633 May 2009.
- [16] Casati E., Colonna P., Nannan N.R. Supercritical ORC Turbogenerators Coupled with Linear Solar Collectors. 30th Ises Biennial Solar World Congress 2011, Swc 2011-2011, Volume 5, pp 4056-4067.
- [17] Barbazza L., Pierobon L., Mirandola A., Haglind F. Optimal design of compact organic Rankine cycle units for domestic solar applications. *Thermal Science* 2014;18:811-822.
- [18] Angelino G., Colonna P., Multicomponent Working fluids for organic Rankine cycles (ORCs). *Energy* 1998;23:449-463.
- [19] Chys M., Van Broek M., Vanslambrouck B., de Paep M. Potential of zeotropic mixtures as working fluids in organic Rankine cycle. *Energy* 2012;44:623-632.
- [20] Young-Jin B., Minsung K., Ki-Chang C., Youg-Soo L., Hyung-Kee Y., Power enhancement potential of a mixture transcritical cycle for a low temperature geothermal power generation. *Energy* 2012;47:70-76.
- [21] HFCs, the Montreal Protocol and the UNFCCC. Bangkok climate change Conference, August-September 2012.
- [22] F-Chart Software Official website. Available at: <<http://www.fchart.com/>>. [accessed 24.02.2015].
- [23] Forristal R., EES heat transfer model for solar receiver performance. Proceedings of SEC, Solar 2004; 2004 July 11-14; Portland, Oregon.
- [24] Dudley V., Kolb G., Mahoney A.R., Mancini T., Matthews C., Sloan M., Kearney D., Test results SEGS LS-2 Solar collector. Albuquerque, Sandia; 1994 Dec. Technical Report No.: SAND94-1884.
- [25] Duffie J.A., Beckman W.A. *Solar engineering of thermal processes* fourth edition, New York, NY: John Wiley and sons.
- [26] Oakdale Engineering Official website. Available at: <<http://www.oakdaleengr.com/>>. [accessed 12.02.2015].

- [27] Quoilin S., Orosz M., Hemond H., Lemort V., Performance and design optimization of a low-cost solar organic Rankine cycle for remote power generation. *Solar Energy* 2011;85:955-966.
- [28] Patnode M. Doctoral Thesis Simulation and Performance Evaluation of Parabolic Trough Solar Power Plants. University of Wisconsin-Madison; 2006.
- [29] Stodola A., Dampf- und Gasturbinen: Mit einem Anhang über die Aussichten der Wärmekraftmaschinen. Berlin, Germany: Springer Berlin; 1922.
- [30] Haglind F., Elmegaard B., Methodologies for predicting the part-load performance of aero-derivative gas turbines. *Energy* 2009;34(10):1484-1492.
- [31] Schobeiri M., Turbomachinery flow physics and dynamic performance. Berlin, Germany: Springer Berlin; 2005.
- [32] CR – Innovation inside, Technical brochure from Grundfos official website. Available at: <<http://www.grundfos.com/products/find-product/CR-CRE-CRN-CRNE-CRI-CRIE-CRT-CRTE.html#brochures/>>. [accessed 24.02.2015].
- [33] Astolfi M., Romano M.C., Bombarda P., Macchi E., Binary ORC (Organic Rankine Cycles) power plants for the exploitation of medium-low temperature geothermal sources - Part B: Techno-economic optimization. *Energy* 2006;66:435-446.
- [34] Radermacher R., Hwang Y. Vapor Compression Heat Pumps with Refrigerants Mixtures Taylor and Francis; 2005.